Environmental Pollution 386 (2025) 127283

Contents lists available at ScienceDirect

Environmental Pollution

journal homepage: www.elsevier.com/locate/envpol

The sanitation in restrooms to respiratory health: modelling concentration distribution changes of bioaerosols across buildings with/without semi-open settings☆

Ting Zhang [b], Zuming Wang [a], Simeng Zhang [a], Yuying Chen [a], Guiying Li [a,*], Taicheng An [a]

[a] *Guangdong-Hong Kong-Macao Joint Laboratory for Contaminants Exposure and Health, Guangzhou Key Laboratory of Environmental Catalysis and Pollution Control, School of Environmental Science and Engineering, Institute of Environmental Health and Pollution Control, Guangdong University of Technology, Guangzhou, 510006, China*

[b] *College of Civil Engineering, Liaoning Technical University, Fuxin, 123000, China*

A R T I C L E I N F O

Keywords:
Restroom bioaerosol
Atmospheric diffusion modelling
Pollution profiles
Respiratory health risk

A B S T R A C T

The sanitation of buildings raises concerns due to pathogen release from restrooms. Herein, bioaerosol pollution profiles from buildings' public restrooms with/without semi-open settings were comparatively analyzed in two cities of China. For the GD building in Southern China with semi-open setting restrooms, the cultivable microbial concentration (C_{bio}) peaked on 2.1–3.3 μm particles (483–1107 CFU/m^3) during the evening with high RH (90 %). Furthermore, the lower the floor, the higher the C_{bio} on 2.1–3.3 μm particles. For the LN building in Northern China without semi-open setting restrooms, the C_{bio} peaked on 1.1–2.1 μm particles (554–907 CFU/m^3) during the evening with low RH (20 %). What's more, C_{bio} was also high (212–389 CFU/m^3) on the finest particle (0.65–1.1 μm). However, the C_{bio} on each particle size was the highest at the 1st-floor for both buildings. Furthermore, the bioaerosol abundances of the genera *Sphingomonas*, *Bacteroidetes*, *Pseudogracilibacillus*, *Cerasibacillus*, *Escherichia Shigella*, *Curvularia*, and *Aspergillus* diffused in restrooms' air. In the >4.5-m corridor to restrooms, airborne *Staphylococcus epidermidis*, *Staphylococcus aureus*, *Bacillus amyloliquefaciens*, and *Aspergillus fumigatus* were abundant along the passages. A mathematical model showed that breathing in 0.65–3.3 μm bioaerosols from restrooms dispersing to outdoor architectural complexes increased health risks. A wind tunnel test explicated that 0.2–2.5 m/s winds of 65 %–90 % RH in the GD building increased 0.3–1.5 m horizontal diffusion concentration gradients of deposited cultivable *Escherichia coli* bioaerosols. The modeling highlights the airborne bio-pollutant diffusion-induced inhalation risks from sanitation systems in southern and northeastern cities.

1. Introduction

Approximately 99 % of the global population breathes air exceeding the World Health Organization (WHO) air quality limits (https://www.who.int/news/item/04-04-2022-billions-of-people-still-breathe-unhealthy-air-new-who-data). Intense human hygienic activities intensify a vast range of urban air pollutants and domestic wastes (Zhang et al., 2023b), and 75 % of households are unsatisfied with their sanitation systems, among which "toilet plume" aerosols are the dominant threat (Zhou et al., 2022). People are inevitably exposed to airborne microbes carried by these aerosols (Collings et al., 2023; Violaki et al., 2021), and 5 %–34 % of them have adverse effects on human organs, including lungs, heart, and circulatory system (Kim et al., 2018). Therefore, understanding how bioaerosols are transported in various restroom environments within buildings has aroused international interest (Erath and Ferro, 2022).

The diffusion, transmission, and settling of emitted bioaerosol from public restrooms of buildings in cities are complicated (Ali et al., 2022). Some bio-pollutants prefer to travel long distances and settle on surface of various substrates (Chen et al., 2024a). Certain outdoor microparticles, when combined with indoor airborne microbes in different seasons, can alter indoor air quality on each floor of high-rise buildings due to wind-induced pressure differences in different geographical regions (Fu et al., 2021; Huyen et al., 2024). During COVID-19 pandemic, buildings

☆ This paper has been recommended for acceptance by Pavlos Kassomenos.

* Corresponding author.
E-mail address: ligy1999@gdut.edu.cn (G. Li).

https://doi.org/10.1016/j.envpol.2025.127283
Received 28 July 2025; Received in revised form 27 September 2025; Accepted 15 October 2025
Available online 17 October 2025

with public transport indoor settings have bioaerosol transmission problems (Braggion et al., 2023). One possible reason is that tiny airborne microbes can stay alive (either active or inactive) for a long time and stick to particles as they move, raising unknown risks (Gollakota et al., 2021). For instance, wind-induced seasonality is confirmed for resuspended ^{137}Cs from soil dust and bioaerosols near the Fukushima Dai-ichi nuclear power plant (Ota et al., 2023). Understanding of climate impacts on the diffuse bioaerosol pollution changes around the cities' building public sanitation areas has not been realized.

Bioaerosols may resuspend in indoor-outdoor air of restrooms (Liu et al., 2023), but it is difficult to characterize their pollution profile owing to insufficient considerations of impacts of meteorological parameters (Qi et al., 2018; Xie et al., 2018). Outdoor wind speed of 2–4 m/s accelerates indoor pollution across many unknown trajectories, leading to improper evaluation of secondary releases of bioaerosols from some sources like garbage bins (Dong et al., 2024; Li et al., 2021). To date, it is still unclear if outdoor meteorological conditions can improve indoor air quality (Sui et al., 2021). Few buildings address operation, maintenance, and retrofitting, and most do not focus on airborne pathogen transmission (Morawska et al., 2024). The amount of dust carried by street canyon wind shows a complicated relationship with PM_{10} levels on humid days; especially in semi-arid areas, both relative humidity (RH) and wind speed are connected to these predictions (Csavina et al., 2014; Ravi and D'Odorico, 2005). Therefore, a practical study on building street zone modelling on the diffuse bioaerosol distribution characteristics around public building restrooms is necessary.

Besides, there are unknown dispersion differences between bacteria and fungi under indoor-outdoor air exchange environments (Megahed and Ghoneim, 2021; Myers et al., 2021). Some researchers claim that the main source of microbes indoors in various buildings is from outdoors (Guo et al., 2021; Tseng et al., 2011), where bioaerosols penetrate indoors through natural ventilation (Guyot et al., 2018; Lewis et al., 2023). In an individual apartment, 16.5 % of indoor bacteria are reported from outdoors (Miletto and Lindow, 2015). A mass balance calculation indicates 70 % of indoor fungi and 80 % of airborne allergenic fungal taxa being associated with indoor emissions rather than outdoor contribution from ventilation (Zhang et al., 2023a). Furthermore, urban architectural composition and building structures are a key affecting factor; for example, building closed or semi-open settings (e.g., hanged walls) and building coverage ratios, which vary from northern city to southern city, affect air pollutant transmissions in the canyon winds (Liu et al., 2022). In a room plan with a minimum connection with the façade, certain areas of the indoor areas, such as the washing room, passages, and working room, are connected, allowing for fluid movement. Therefore, it is urgent to determine how bioaerosols will disperse in restrooms of buildings with semi-open settings under cities' weather conditions.

To explore the bioaerosol characteristic effects on indoor air qualities in city public building sanitation systems and thereby risks, herein, this study investigated (1) two seasonal distribution characteristics of bioaerosol concentrations, sizes, and communities from restrooms to passages with/without semi-open spaces (hanged walls) of buildings of two southern and northern cities through on-site monitoring; (2) influence principles of bioaerosol diffusion under humid wind conditions using a wind tunnel test; and (3) the predicted concentration distribution of bioaerosols in the air of crowded- and sparse-building complexes using a computational fluid dynamics (CFD)-aided model simulation for regional areas. This work is devoted to a comparative quantification of pollution characteristics of bioaerosols that resulted in human exposures from public restrooms of building complexes on humid days of the subtropical monsoon city in South China and non-humid days of a warm city in Northeast China. The modelling study strengthens the methodology for public hygiene pollution prediction for risk management in the urban environments.

2. Materials and methods

2.1. Study sites and sample collection

The study was comparatively conducted of two seven-floor university buildings (GD and LN) in two typical cities in China. The GD with semi-open settings (113°24′44.57″E, 23°2′24.10″N) is located in Guangzhou, South China, which has a humid subtropical climate, with hot and humid summer but mild winter. There are one male and one female restroom on each floor under natural ventilated conditions (Fig. S1). Each restroom (indoor length × width × height: 7.7 m × 4.1 m × 2.7 m, room volume was 75 m^3) has five small compartments with squat toilets. The sampling sites include the center of restrooms and 2 m outside of restroom doors (hall areas outdoor semi-open hall: 7.8 m × 2.2 m × 2.7 m). Floors 1 to 7 are connected by a vertical staircase, which is flanked by the halls on one side and the outdoor area on the other. A total of 42 bioaerosol samples were collected in the morning (8:00–9:00 a.m., before working activities) and evening (8:00–9:00 p.m., after working activities) during summer and winter time.

The LN without semi-open settings (121°41′24.02″E, 42°2′35.40″N) is located in Fuxin, Northeast China, which features a semi-arid continental monsoon climate and four distinct seasons with cold and dry winter. Similarly, there are one male and one female restroom on each floor under natural ventilated conditions. Each restroom (indoor length × width × height: 8.6 m × 4.1 m × 2.9 m, room volume was 67 m^3) has five to eight small compartments with squat toilets. There is an indoor circle-closed hall (11.6 m × 9.1 m × 2.9 m) outside of the restrooms on each floor. A total of 42 bioaerosol samples were also collected in the morning and evening during winter time.

Bioaerosols were collected on-site using an Andersen six stage air sampler for viable bacteria (Aiwo Environmental Devices Co., Ltd., China) for 3 min at 28.3 L/min. Samplers were cleaned with alcohol before and after use in each scenario. The nutrient agar plate (NAP) was used for total cultivable bacteria and fungi. The blood agar plate (BAP) was crucial for differentiating a wide range of pathogens, which are difficult to grow due to the enriched nutrient composition, making it an insight into pathogenic potential and microbial behavior in the air samples of this study. Colonies formed at 37 °C for 12–72 h were counted for cultivable bioaerosol detection by NAP and BAP, respectively.

Meanwhile, total bioaerosols were sampled with the sterilized mixed cellulose ester microporous membrane (0.22 μm) (Guangdong Huankai Microbial Sci. & Tech. Co., Ltd.), using the Andersen six stage air sampler. Membranes were used to extract DNA. The V3–V4 region of bacterial 16S rRNA and the Internal Tran-scribed Spacer (ITS) region of fungi were amplified (Chen et al., 2024b). High-throughput sequencing was performed using the PacBio Sequel II platform. The raw sequence information was uploaded to the NCBI Short Read Archive.

Herein, eight sample sites (FE, FM, LE, LM, MWCM, MWCE, WCE, WCM) were presented. The FE, LE, MWCE, and WCE represent the sites near the garbage bins (F), in the hall (L), in the male restroom (MWC), and in the female restroom (WC), respectively, detected in the evening (E). The FM, LM, MWCM, and WCM represent sites near the garbage bins, in the halls, in MWC, and WC, respectively, and were detected in the morning (M).

Further, the meteorological covariates, including wind speed, temperature and atmospheric RH, and sampling data in the seasons were on-site measured. The indoor ventilation situation of the buildings was counted as the averaged 1.5 m-height wind speed of the restrooms and halls in the morning and evening, measured with the wind speed meter. The detailed information is presented in Table S1.

2.2. Wind tunnel tests

Airborne bioaerosol diffusion was experimentally simulated using a patented wind-tunnel (1.5-m straight wind tunnel involving an oblique diffusion tube, wind blower and accessories) to provide the dataset for modelling. *E. coli* liquid (1×10^5 cells/mL) was aerosolized using a medical atomization device (Yuwell Medical Equipment & Supply Co., Ltd., 403M) from an inlet located at the end of the 1.6-m tube, which was simulated as the emission source. Andersen bioaerosol samplers were placed at the 50-, 90-, and 150-cm distances from the source (Fig. S2). The cultivable *E. coli* concentration (C_{bio}) was measured to analyze deposition and diffusion profiles of the bioaerosols released by the axial flow fan pipeline exhaust fan (250 mm, 1450 rpm). Moreover, the results can validate and explicate the facts of the horizontal diffusion profiles of bioaerosols under humid wind conditions.

2.3. Dataset setups and modelling

The built-up areas were modeled of buildings with complex shapes, functionalities and construction characteristics. City information model-based CFD simulation schemes were conducted based on the geographical information system (GIS) information and building geometrical dataset (Fig. S3), involving data collection, scenario dataset establishment, and results output. Through a regional island GIS-CFD model, the computational grid of 1,247,666 tetrahedral cells with the mesh size of 20 was refined around the boundaries and bacterial source. A k-Ω turbulence model with low-Re correlation and curvature correction was used. Scale-resolving simulation setup was defined. A set of scenarios with air flow regimes (Scenario A and B) was applied (Fig. S1).

Ambient bioaerosols were simulated as the discrete phase, and air was simulated as the continuous phase in a discrete phase model (DPM). Within bioaerosol emission regime A, the natural ventilation supply air inlet is defined as a velocity profile and presented as a zero-pressure boundary. Within bioaerosol emission regime B, the velocity boundary condition on each side of buildings is defined as a zero-pressure boundary, with 1.25 m/s wind speed and 50 % RH setting by 0.01 % water vapour percentage in air. Mean diameter of bioaerosol was set as 2.5 μm in a rosin-ramler diameter distribution range of 6.5×10^{-7}–1.0×10^{-5} m (mean: 2.5×10^{-6} m), while the number of diameter and the spread parameter was 10 and 3.5, respectively. In boundary condition setups of turbulent dispersion of bioaerosols, the discrete random walk model and radon eddy lifetime were adopted, with the time scale constant as 0.15. Moreover, the rough wall model was chosen, and nonspherical drag low and 0.75 shape factor were used and the particle rotation was considered using Dennis-et-al rotational drag law and Oesterle-Bui-Dinh Magnus lift law model. Regime A (typical weather situation with low building density in a case area) and regime B (same case area with high building density) were simulated using GIS-CFD-aided regional modelling. To present bioaerosol concentration distributions, weather conditions were weak wind and high RH. The following were the specific settings for both scenarios:

Scenario A: The flush event-induced bioaerosols were emitted in restroom with a building on an island with a low density of building coverage ratio (≈3 %).

Scenario B: The flush event-induced bioaerosols were emitted in a megacity area with buildings on an island with an increased density of building coverage ratio (≈15 %).

The emission source was the toilets' outer wall windows, turbulent intensity and turbulent viscosity ratio were 5 % and 10. Referring to the on-site monitored wind speed and temperature in GD, the total flow rate of bioaerosols was set as 5×10^{-9} kg/s, temperature was 298 K, and velocity magnitude was 0.25 m/s. Then, the numerical simulation was conducted with the time step size of 0.01 s, the number of time steps of 30,000, and the simulation period reaching 0–300 s.

3. Results

3.1. Bioaerosol pollution profile results in the building with/without semi-open settings

3.1.1. Concentration distribution of bioaerosol in humid air

Fig. 1a presents the culturable bioaerosol concentration and size distribution in the female toilet ((W)WC) and outside toilets (halls) of 1st- and 7th-floor of the GD building over a whole day in summer. To explore air quality in sanitation areas of floors 1–7 in the GD building in Southern China, average concentrations of airborne cultivable microbes (C_{bio}) of the male toilet (MWC) were comparatively analyzed. In daytime (RH: 80 %), total C_{bio} on all particle at the 1st- and the 7th-floor were 525 and 189 CFU/m^3, respectively. C_{bio} increased first and then decreased with the increased particle size but peaked differently (2.1–3.3 μm at 1st-floor and 7th-floor (130 and 71 CFU/m^3). At nighttime (RH: 65 %), the total C_{bio} on all particles was slightly different between the 1st- (600 CFU/m^3) and 7th-floor (566 CFU/m^3). Furthermore, the highest C_{bio} (306 and 236 CFU/m^3 at 1st- and 7th-floor, respectively) was at finer particles (1.1–2.1 μm) in nighttime. In daytime (RH: 80 %), the C_{bio} on 1.1–2.1 μm sized particles was 118 and 35 CFU/m^3 at 1st- and the 7th-floor, respectively. These demonstrate high differences of C_{bio} between daytime and nighttime in GD building, and inhalable bioaerosol increased in passages, especially at nighttime.

Fig. 1b presents the atmospheric bioaerosol diffusion characteristics in different sanitation areas and bioaerosol distributions in MWCs, WCs, and halls at 1st- and 7th-floor in the GD building. In daytime (RH: 80 %), at 1st-floor, C_{bio} reached 919, 1643, and 566 CFU/m^3 in MWC, WC, and halls, respectively. Comparatively, much lower of C_{bio} were found at 7th-floor with 377, 341, and 189 CFU/m^3 in MWC, WC, and hall, respectively. Specifically, at 1st-floor, the most abundant bioaerosol was on fine particles (1.1–2.1 μm (353 CFU/m^3), 2.1–3.3 μm (518 CFU/m^3), and 1.1–2.1 μm (236 CFU/m^3) in MWC, WC, and halls, respectively). In contrast, at 7th-floor, the most abundant bioaerosol was on large particles (2.1–3.3 μm (165 CFU/m^3), 4.7–7.0 μm (118 CFU/m^3), and 2.1–3.3 μm (71 CFU/m^3) in MWC, WC, and halls, respectively). These results demonstrate that higher concentrations of bioaerosol generated in MWCs and WCs can horizontally diffuse to the halls in daytime (RH: 80 %) through natural ventilation in summer because of the semi-open setting design of the GD building.

Comparatively, Fig. 1c demonstrates higher bioaerosol concentrations in restrooms and halls under humid or less humid air situations, which were found on 1st-floor (MWC, WC, Hall C_{bio}: 907, 682, 601 CFU/m^3) than on those 7th-floor (MWC, WC, Hall C_{bio}: 613, 518, 778 CFU/m^3) in the summer nighttime (RH: 65 %). Further, the C_{bio} was peaked on finer particles in the nighttime than daytime, and C_{bio} on finer particles (1.1–2.2 μm) in the nighttime was higher. The possible reason is also that water evaporation might occur on the airborne particles, decreasing the particle size in nighttime (Božič and Kanduč, 2021; Kraus et al., 2025). The particle size distribution characteristics significantly proved horizontal diffusion of bioaerosol from restrooms to the halls since finer particles can suspend in air for long-distance transport (Chu and Yang, 2022).

Further, Fig. 1d comparatively analyzes the average C_{bio} of MWC, WC and halls of 1st-, 4th-, and 7th-floor in summer and winter. The average C_{bio} increased first, peaked at 2.1–3.3 μm, and then decreased with increased particle size, although average C_{bio} in almost all particle sizes except 0.65–1.1 μm was higher in summer than winter. Total C_{bio} in all particle sizes soared to 4818 CFU/m^3 in summer, presenting 8.5 times of those concentrations in winter. Particularly, in 3.3–4.7, 2.1–3.3, and 1.1–2.1 μm particles, the average C_{bio} in summer were 836, 2933, and 754 CFU/m^3, which were 7.9, 22.6, and 9.2 times higher than those in winter. It is because low average temperature and RH during wintertime are unfavorable for microbial growth (Ghosh et al., 2015). Furthermore, the microbes occurring inside people have adapted to survive at typical human body temperatures (30°C–40 °C). As such, few

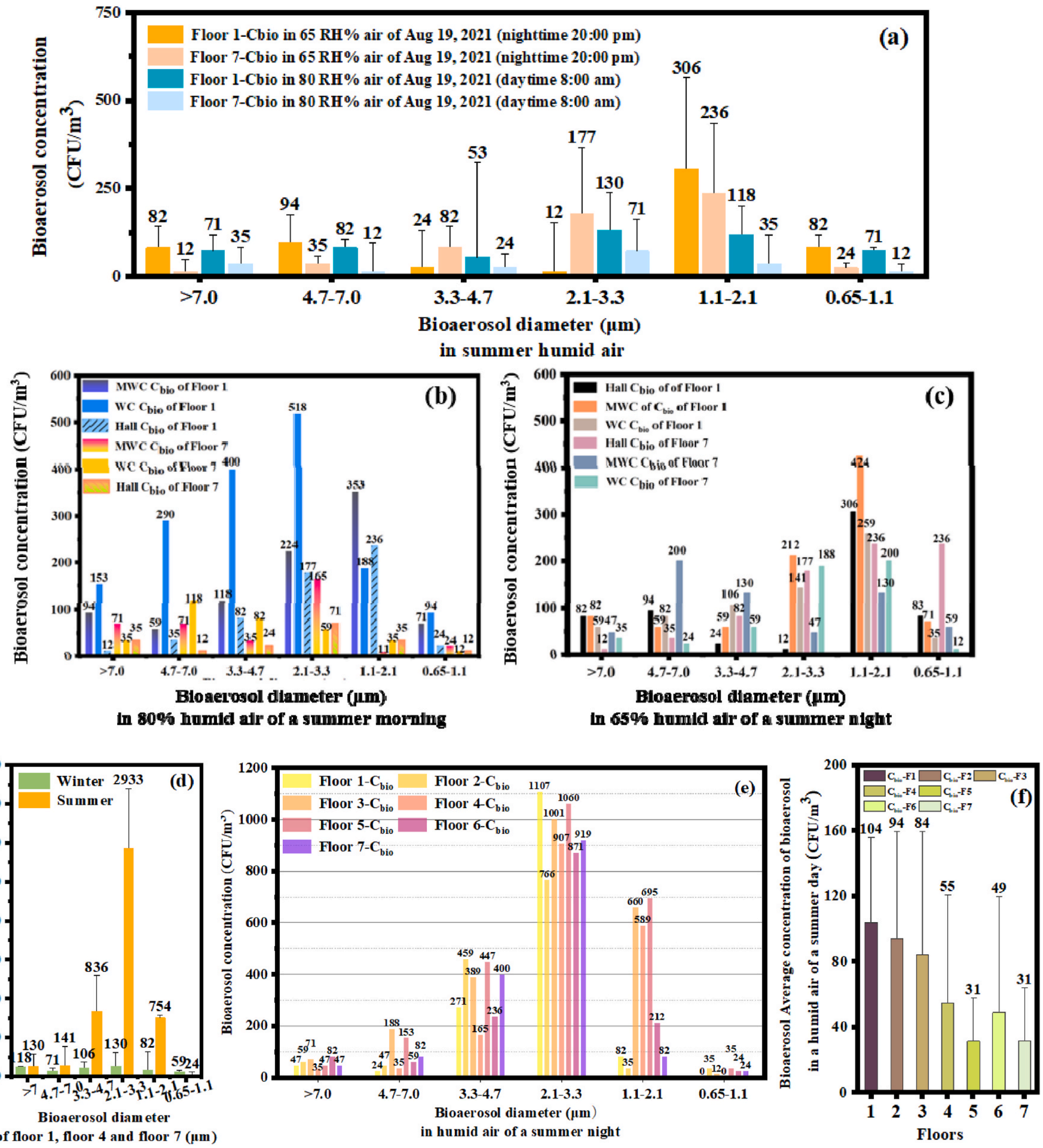

Fig. 1. On-site monitored culturable bioaerosol concentration and diameter characteristics in horizontal (Restrooms to halls in each floor) and vertical direction (Restrooms from 1st- to 7th-floor of GD building). Bioaerosol distributions (a) at daytime and nighttime, (b–c) in the man restrooms, the woman restrooms, and the halls of the summer nighttime and daytime, (d) in summer and winter, and (e) at the lower floor and the upper floor halls (1st-to 7th-floor), and (f) at seven floors on a humid day in summer.

microbes can survive in bioaerosols and some may enter a dormant state due to the harshness for them (Gupta et al., 2021). All information indicates that seasonal emission diffusion in Southern China buildings with open settings can be affected by seasonal meteorological scenarios and the potential inhalation health risk is high in summer.

As Fig. 1e shows, in the humid air of a summer night, total C_{bio} in the halls adjacent to MWC and WC from the 1st-to 7th-floor was 1531, 1401, 2321, 1731, 2437, 1484, and 1554 CFU/m^3, respectively. Furthermore, the most abundant bioaerosols were on 2.1–3.3 μm particles in all halls. The 2.1–3.3 μm C_{bio} from the 1st- to 7th-floor was 1107, 766, 1001, 907, 1060, 871, and 919 CFU/m^3, accounting for 72 %, 55 %, 43 %, 52 %, 43 %, 59 %, and 59 % of total bioaerosol in all particle sizes, respectively. That is, air quality in the 1st-floor hall adjacent to MC and WMC was incredibly unsatisfactory owing to abundant inhalable bioaerosols.

Furthermore, Fig. 1f shows that the average concentration of airborne bioaerosol (0.65–>7 μm) of the decreasing characteristics at 1st- to 7th-floor was significant on a humid summer day in the GD building. In a building, the possible vertical dispersion of bioaerosol in the humid summer became a critical issue. These results demonstrate that vertical bioaerosol diffusion dominantly affects air bio-pollution in the seven-floor building with semi-open settings on the humid days. A light breeze with low speed may occasionally limit vertical movement with deposition a few meters away from the source (Obayori, 2023).

3.1.2. *Diffused bioaerosol community*

Fig. 2 presents the microbial community of diffused bioaerosols in the GD building. The bacterial bioaerosol OUT numbers fluctuated slightly between 1077 and 1547 at the eight sample sites (FE, FM, LE, LM, MWCM, MWCE, WCE, WCM), including the wash closet halls, the rubbish bins, and the man-used and woman-used wash closets in the sampling periods of evening and morning, respectively. The highest bacterial bioaerosol OUT number of 1547 was at WCE (female restroom

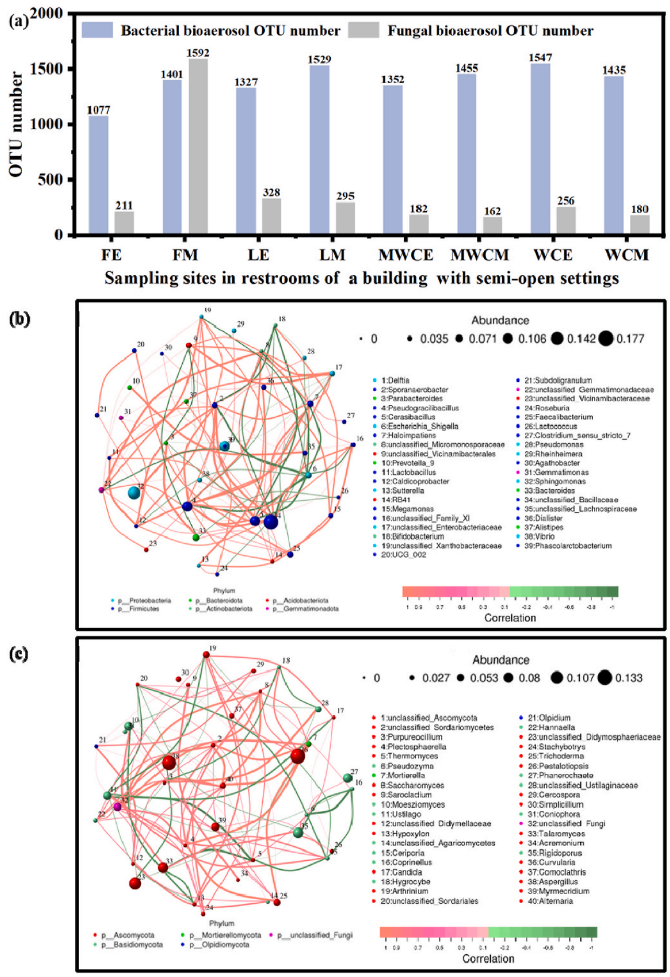

Fig. 2. (A) Airborne bacterial and fungal bioaerosol OTU number; (b) association analysis of top 40 bacteria genera; (c) association analysis of top 40 fungi genera.

in the evening). Comparatively, the fungal bioaerosol OUT numbers also fluctuated slightly between 162 and 328 and were much lower than those of bacterial bioaerosol OUT numbers except at FM site (near garbage bins in the morning). At FM site, the fungal bioaerosol OUT number was very high (1592), which was even higher than those of bacteria at all sites. These indicate that bacterial community diversity was generally higher than that of fungi at most sites except at FM site, where fungal community diversity was very high probably due to higher enrichment of some fungi and shaping specific microbial community functions during garbage decomposition (Lin et al., 2023; Yu et al., 2021). Atmospheric bioaerosol diffusion may deliver human pathogens from restrooms to halls, impacting the sanitary quality of the whole building. Therefore, the diverse bacterial and fungal community in the restrooms with garbage bins should be paid more attention.

The genus bacterial bioaerosol network of the above eight samples in GD case is shown in Fig. 2b. The highest abundant genus bacterium was unclassified_*Bacillaceae* (0.177), followed by *Sphingomonas* (0.142). The strains of *Bacillaceae* family possess high growth rate, easy cultivation, and strong environmental resistance (Ren et al., 2023), enabling them to widely live in soil, water, air, and animal intestines (Fang and Ning, 2024). High abundance of them may be due to the excretion of urine and faeces in this study. The genus fungal bioaerosol network of the above eight samples is presented in Fig. 2c. The highest abundant genus fungi were *Curvularia* and *Aspergillus* with 0.133 abundance. *Curvularia* is a genus with a worldwide distribution, and some of which are opportunistic pathogens of humans, causing cutaneous, cerebral, respiratory tract, and corneal infections (Marin-Felix et al., 2020). Furthermore, similar cultivable pathogenic bacteria were detected in the restrooms of the GD building and the LN building, including *Staphylococcus aureus* and *Staphylococcus lugdunensis* (Tables S2 and S3), implying the atmosphere diffused pathogen hazards in the Southern and Northeastern China buildings.

3.1.3. Comparative analysis on bioaerosol pollution profiles in GD/LN building

To explore environmental factors (e.g., atmospheric RH, building structure, density, and location) impacting bioaerosol diffusion-induced risks, the temporal-spatial scaled bioaerosol pollution profile of the GD building (with semi-open settings in Southern China) was compared to the LN building (with closed restrooms in Northeast China).

The bioaerosol pollution profiles of these buildings at 1st-, 4th-, and 7th-floor were compared at different atmospheric RH (Fig. 3a). For the GD building, the C_{bio} peaked on 2.1–3.3 μm particles (483–1107 CFU/m^3) during the evening with high RH (90 %). Furthermore, the lower the floor, the higher the C_{bio} on 2.1–3.3 μm particles. Comparatively, for LN building, the C_{bio} peaked on 1.1–2.1 μm particles (554–907 CFU/m^3) during the evening with low RH (20 %). What's more, the C_{bio} was also very high (212–389 CFU/m^3) on the finest particle (0.65–1.1 μm). These indicate that inhalation exposure risks of bioaerosols related to restrooms are also high, especially at lower floors for both styles of buildings. Therefore, in indoor air environments, humid wind may enhance denser and larger bioaerosol deposition on the lower floor of buildings with semi-open settings, while lack of ventilation may lead to high bioaerosol concentration in closed restrooms with low RH.

Examining human health risk due to bioaerosol exposure from human activities is necessary for public hygiene controls (Douglas et al., 2018). Therefore, total cultivable bioaerosols and pathogenic bioaerosols were detected during wintertime (Fig. 3b–c). In LN case, total culturable (2226 CFU/m^3) and pathogenic (2733 CFU/m^3) bioaerosol concentrations peaked on 1.1–2.1 and 0.65–1.1 μm particles, respectively. Comparatively, both total culturable and pathogenic bioaerosol concentrations at almost all particle sizes were much higher than those in GD case. Further, the particle size distributions of them were different, with even distributions at different particle sizes in GD case. Total culturable bioaerosol (130 CFU/m^3) peaked on 2.1–3.3 μm, and pathogenic bioaerosol (47 CFU/m^3) peaked on 1.1–2.1 and 3.3–4.7 μm in GD case.

Furthermore, the spatial distribution features of bioaerosols in LN case were specifically investigated due to higher potential health risks. For total culturable bioaerosol, the average concentration was 1.3-time higher at 1st-floor than at 4th-floor, and most culturable bioaerosol at all floors peaked on 1.1–2.1 μm particles (Fig. 3d). For cultivable pathogenic bioaerosols, highest average concentration (93 CFU/m^3) was on 0.65–1.1 μm particles at 1st-floor. The culturable pathogens accounted for >68 % of total culturable bioaerosol, and most culturable pathogens at all floors also peaked on this particle size (Fig. 3e). These indicate that inhalation exposure risk is very high in LN case especially at the 1st-floor due to more pathogens on finer particles. The finer the particles, the greater the potential to be inhaled into lower airway of humans, triggering respiratory diseases like asthma and chronic obstructive pulmonary disease (Pöhlker et al., 2023; Wang et al., 2021). In GD case with semi-open settings, most pathogens attached on larger particle (2.1–3.3 μm) and about 27 % of total bioaerosol were pathogens (Table S2). Comparatively, in the LN building, about 43 % of total bioaerosol were pathogens, including *Staphylococcus aureus*, *Staphylococcus epidermidis* and *Aspergillus fumigatus* (Table S3). Therefore, the potential inhalation risks to pathogenic bioaerosol deserve greater concern in both closed restrooms (due to more pathogens of finer <1.1 μm particle) and semi-open closed restrooms (due to higher concentration of pathogens on larger 2.1–3.3 μm inhalable particle) especially at lower floor. However, the underlying mechanisms of the diffuse bioaerosol pollution in the sanitation environment is less known.

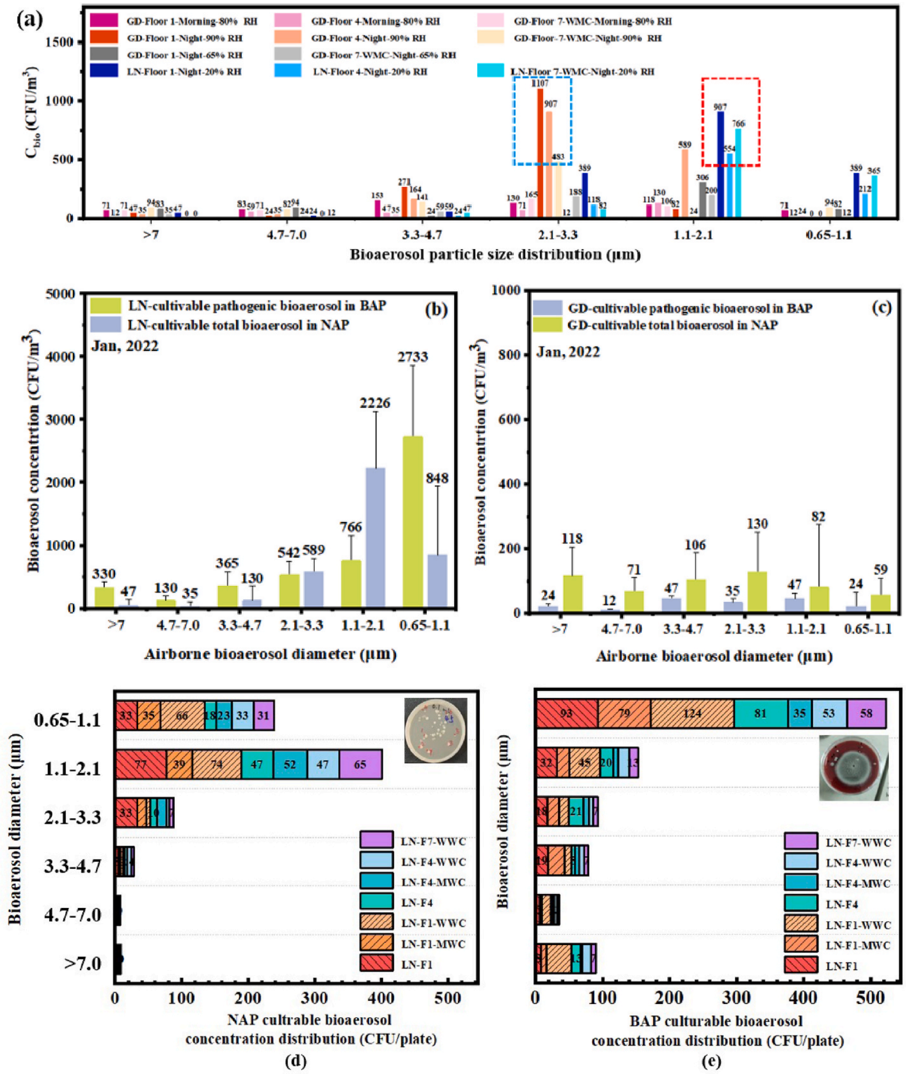

Fig. 3. Culturable bioaerosol particle size distribution and concentration in compared campus building of China. (a) C_{bio} in the floors of two buildings, two seasons, two cities, and different atmospheric RH. Total culturable bioaerosol concentration and pathogenic bioaerosol concentration in the building of (b) LN, (c) GD, and (d) culturable bioaerosol diffusion concentration by NAP, (e) pathogenic bioaerosol diffusion concentration by BAP in LN at different floors.

Furthermore, regression analysis was performed to demonstrate size distribution differences of bioaerosols in GD and LN buildings. These equations of bioaerosol cutting size (x) and concentration (y) were listed. As Fig. S4 shows, y values of finer cutting sizes (<1 μm) increased in LN buildings, which are related to the building structures without open settings. The y values in GD buildings with open settings were relatively low, but the 2.5 μm inhalable bioaerosol concentrations were relatively high, indicating the potential inhalation exposure risks.

3.2. *Influence principles of bioaerosol diffusion under humid wind conditions*

Further, Fig. 4 presents the effect of atmospheric RH on bioaerosol transmission adopting the wind-tunnel-based *E. coli* bioaerosol concentration measurement (initial concentration: 1×10^5 CFU/m^3). The effects of wind speed on bioaerosol diffusion with RH 50 %–55 % are illustrated in Figs. 4a–b. With 0.2 m/s wind speed, total *E. coli* bioaerosol diffusion concentrations at all particle sizes were 2402, 931, and 1284 CFU/m^3 at 50, 90, and 150 cm diffusion distances, respectively. With 2.5 m/s wind speed, total *E. coli* bioaerosol diffusion concentrations at all particle sizes were 1461, 1049, and 343 CFU/m^3 at 50, 90, and 150 cm diffusion distances, respectively. Further, the vast majority of bioaerosol attached on finer particle (0.65–1.1 μm) in these cases. It is because, at lower RH, water evaporation might occur on airborne particles during diffusion, decreasing the particle size (Božič and Kanduč, 2021; Kraus et al., 2025). These demonstrate that higher speed wind velocity significantly dilute source emitted larger sized bioaerosol (3.3–7.0 μm), while finer sized bioaerosol (0.65–1.1 μm) could be easily dispersed in air for a longer period. However, the inhalable bioaerosols (1.1–2.1 μm) disperse and accumulate in the air by relatively strong wind (2.5 m/s), resulting in higher air pollution.

Figs. 4c–d illustrate the effect of RH on *E. coli* bioaerosol diffusion with 0.2 m/s wind speed to simulate a natural ventilation situation. With a relatively high RH (65 %), *E. coli* bioaerosol diffusion concentration was 965, 977, and 685 CFU/m^3 at 50, 90, and 150 cm diffusion distances, respectively. With extremely high RH (90 %), *E. coli* bioaerosol diffusion concentration was much lower (353, 377, and 542 CFU/m^3 at 50, 90, and 150 cm diffusion distances, respectively). Further, the vast majority of bioaerosol attached onto both finer (0.65–1.1 μm) and larger (>7.0 μm) particles under both conditions. These demonstrate that atmospheric RH affects both natural ventilation-associated bioaerosol diffusion and particle size distribution in air. Higher RH contributed to higher deposition of larger (>7.0 μm) bioaerosols, while lower RH induced a wide size range of bioaerosol deposition. In addition, the

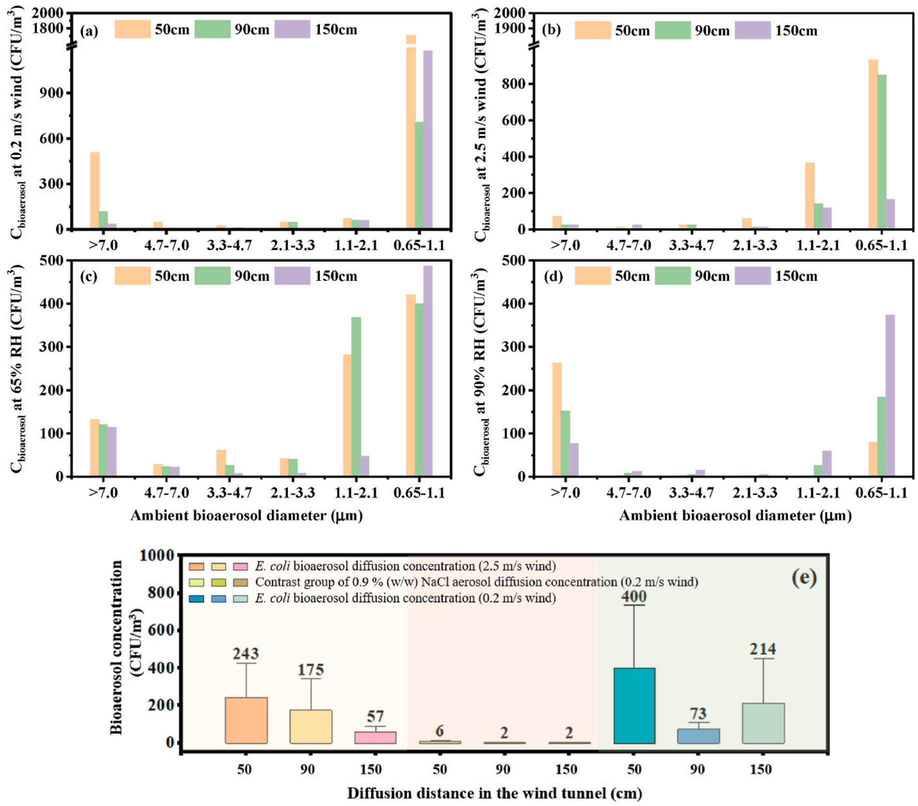

Fig. 4. The wind-tunnel-based *E. coli* bioaerosol diffusion concentration gradients in the scenarios of (a) 0.2 m/s wind speed with 50 %–55 % RH, (b) 2.5 m/s wind speed with 50 %–55 % RH, (c) 65 % RH with 0.2 m/s wind speed, (d) 90 % RH with 0.2 m/s wind speed, and (e) a comparison of concentration with the contrast group of NaCl aerosol.

decreasing concentration gradient of 50–150 cm could be affected by atmospheric RH. Overall, these results highlight significant diffusion of 0.65–2.1 μm bioaerosols in 65 %–90 % RH wind environments, implying higher inhalation exposure risks for remote area residents.

The results of Fig. 4e further demonstrate the environmental scenario effects of wind speeds on pathogenic bioaerosol diffusion concentration gradients, size distribution characteristics, and transmission distances. A good understanding of airflow dynamics in a high temporal and spatial resolution benefits human respiratory health management (Hu et al., 2024). Meanwhile, owing to the humid winds, the pathogenic bioaerosol pollution profiles in the restrooms of the high-rise buildings are different owing to the adhesion ratios of the microbes on the airborne particles in the weather. Then, ambient bioaerosol emissions accompany long-distance transmission, resulting in public residents' exposure potentials to bioaerosols in building complexes, requiring urgent dynamic attention (Mubareka et al., 2019).

3.3. Quantitively modelling results of regional bioaerosol dispersion

Fig. 5 shows the CFD-GIS modelling contours of source-emitted bioaerosol diffusion profiles, while regional building area ratios and the GD building-complex structures-induced bioaerosol diffusion profiles were comparatively considered in the typical meteorological wind scenarios. The atmospheric diffusion ranges of bioaerosols from sources were presented using CFD-DPM simulation, demonstrating that bioaerosols dispersed in outdoor air differed significantly when the building coverage ratio changed. In scenario A with single regime A, when the building structure ratio is low, the atmospheric bioaerosol diffusion range was wide, so bioaerosols could be easily diluted in air along the wind direction (Fig. 5a). However, in scenario B with regime B, when building structure ratio increased, the atmospheric diffusion range decreased at the same discharging time as scenario A (Fig. 5b). It can be deduced that apart from the building structure impacts in cities, airborne bioaerosol could transmit from restrooms to the building complex passage-triggered pathogen concentration distribution changes by building coverage ratios (Table S4) and then accumulate in the GD building surrounding areas. The changed bioaerosol-polluted areas (greater than 1 km^2) of the study suggest that higher building coverage ratios in GD may sometimes lead to an increased risk of exposure.

Regional modelling approaches can be combined as the means of providing a more comprehensive understanding of potential future scenarios of buildings with semi-open settings. Based on these results, the GD structures with semi-open setting and building areas in urban regions have a significant enhancement on the atmospheric diffusion ranges of bioaerosols. The bacterial viability decreased when air pollution occurred and increased when pollution lasted and became severe, owing to the humid air impacts on viable/non-viable bioaerosols.

4. Discussion

4.1. Spatiotemporal influences on bioaerosol concentration in humid air of GD/LN

In this study, the spatiotemporal concentration distributions of restroom aerosols among floors of GD/LN were both evidenced. For example, the highest C_{bio} (306 and 236 CFU/m^3 at 1st- and 7th-floor, respectively) of finer particles (1.1–2.1 μm) in nighttime emerged in GD, while in daytime, total C_{bio} on all particle was 118 and 35 CFU/m^3 at 1st- and 7th-floor, respectively. The study demonstrated the vertical distribution differences of C_{bio} between 1-st and 7-th floor both in the daytime and nighttime. It is because during daytime, bioaerosols are frequently generated during various human activities including restroom flushing, walking, and floor sweeping in indoor restrooms installing squat toilets (Collings et al., 2023; Violaki et al., 2021).

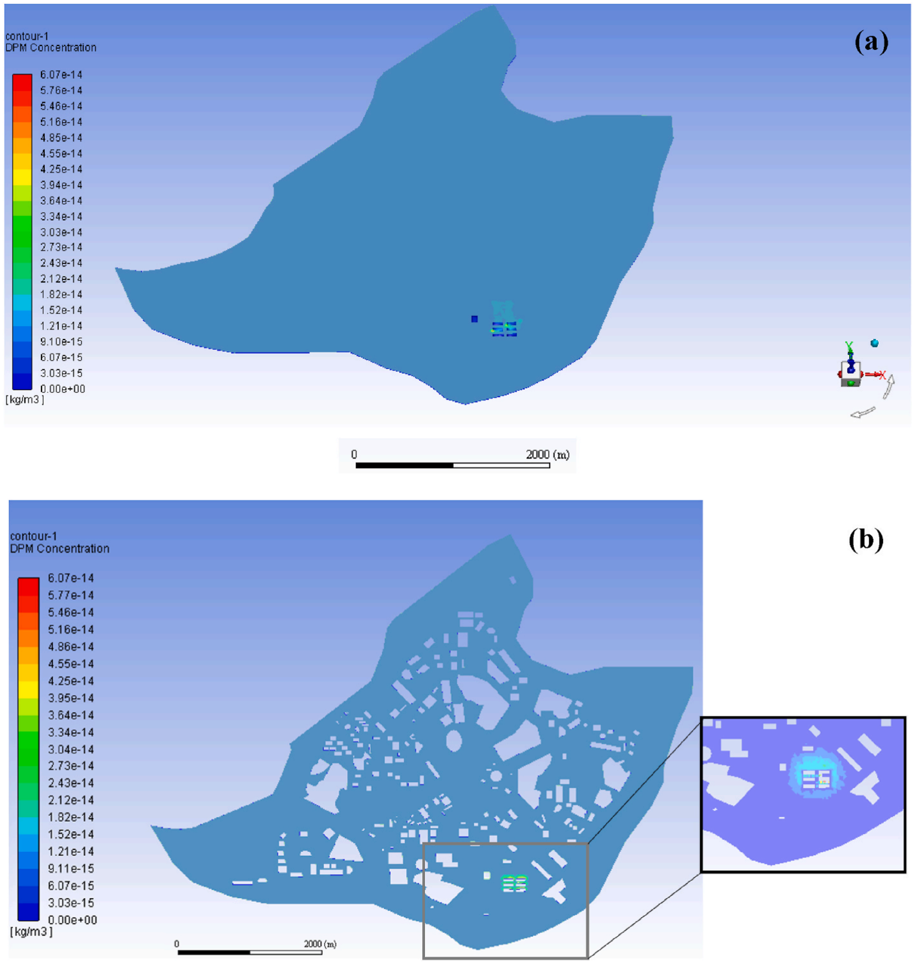

Fig. 5. Modelling forecasting on atmospheric diffusion contours of bioaerosol in an urban building complex area, (a) an island area with low building coverage ratios; (b) an island area with high building coverage ratios.

Generally, total C_{bio} should be much higher in daytime than nighttime. However, unexpected, in this study, much lower values of the total C_{bio} were observed in daytime than nighttime at 7th-floor of the GD building with semi-open settings. Possiblely, in daytime during restroom flushing, lots of droplets are produced with various sizes. Larger droplets are likely to return to adjacent floor limiting their potential for aerosolization due to gravitational sedimentation, but smaller droplets may suspend in atmosphere for pathogen long-distance transport (Pietsch et al., 2018; Wu, 1981). That is, in daytime, many larger droplets and higher RH are resulted from frequent human activities, especially restroom flushing. This also explains the reason why higher C_{bio} was detected on larger particle size in daytime than nighttime. The possible reason for high C_{bio} in nighttime is something other than frequent human sanitation activities, since sampling time delicately avoided human sanitation activity fastigium. We suppose that RH may dominate bioaerosol concentration distribution. In nighttime, less human activities may lead to lower RH, and water evaporation might occur on the airborne particles, decreasing the particle size (Božič and Kanduč, 2021; Kraus et al., 2025). Meanwhile, near-surface air turbulence may resuspend microbes in dust particles or droplets to air (Ota et al., 2023). In addition, we also observed higher total C_{bio} at the 1st-floor than 7th-floor, especially in daytime, meaning that sanitary quality of lower floors is unsatisfied, particularly in summer humid air. It might be that effect of wind to higher floor is stronger than that lower floor, resulting in short discrete plumes of bioaerosols. Moreover, the atmospheric precipitation and increased relative humidity result in a reduction in the number of bioaerosols owing to the generation of giant bioaerosol particles (Barbosa et al., 2022).

Moreover, the horizontal distribution of the inhalable bioaerosol was detected owing to atmospheric diffusion of airborne microbes; for example, the concentration of bioaerosols increased in passages significantly in nighttime by the restroom bioaerosol emissions. The C_{bio} on each particle size was the highest at each floor hall passageway of the floors under humid air conditions, while there was a different variation rule within the GD building. More microbes on finer particles for LN building have also emerged because the water evaporation occurs on the airborne particles at low RH (Božič and Kanduč, 2021; Kraus et al., 2025), and higher RH facilitates microbial growth (Ghosh et al., 2015). Furthermore, high C_{bio} for LN building is due to its closed restrooms, which is unfavorable for bioaerosols owing to a lack of ventilation (Chen et al., 2024b). The worse air quality in restrooms of lower floors and the adjacent passages also presented higher inhalable bioaerosol levels, deserving more concerns and controls due to the long-distance atmospheric diffusion of airborne pathogens from the sources (Zhang et al., 2023b; Zhang et al., 2020).

4.2. Spatiotemporal variation of microbial communities

During the study period, unlike other microbial species in the air of indoor settings, the public restroom microbial community studies explained about the specific taxa, including *Pseudomonas*, *Pseudogracilibacillus*, *Sphingomonas*, *Escherichia_Shigella*, and *Aspergillus*, which are dispersed constantly around buildings from restrooms. The top diffuse bacteria in the restrooms' air included *Bacillaceae*, *Sphingomonas*, *Pseudogracilibacillus*, *Cerasibacillus*, *Delftia*, *Haloimpatiens*, *Megamonas*, *Vicinamibacterales*, *Rheinheimera* and *Escherichia_Shigella*. The top fungi were *Aspergillus*, *Curvularia*, *Talaromyces*, *Phanerochaete*, *Ustilago*, *Moesziomyces*, *Arthrinium*, *Alternaria*, *Trichoderma* and unclassified Fungi. The major bacteria and fungi that form the bioaerosol microbiota, which plays a pivotal role in maintaining microbial community structures, evidently cause human inhalation exposures (Peng et al., 2025).

Sphingomonas is a genus of aerobic, gram-negative bacilli found in moist environments. *Sphingomonas* species are obligate aerobic rod-shaped pathogens as a cause of infections. For instance, *Sphingomonas paucimobilis* can cause atrophic rhinitis (Alyousef et al., 2025), which can colonize everywhere in sanitary fixture settings where water is used (Menekşe et al., 2023). In addition, the 0.106 abundant genus bacteria were *Pseudogracilibacillus* and *Cerasibacillus*, which are present as human gut microbiomes, modulating digestive health and metabolism, and *Delftia* (Anthamatten et al., 2024). The 0.071 abundant genus bacteria included *Escherichia Shigella*, *Bacteroides*, *Haloimphtients*, unclassified *Enterobacteriaceae, Faecalibacterium*, and *Sporanaerobacter*, which have been suggested as the key marker of the healthy gut of healthy human adults (Leylabadlo et al., 2020).

The abundant microbes affect the temporal and spatial variation of communities in the humid air of building restrooms. *Aspergillus* is widely distributed in city water, air, and soil, and is one of the fungi capable of affecting plants, animals, and human health due to their high survivability in extremely difficult environments and their pathogenicity (Ibrahim et al., 2025; Zhang et al., 2025). Furthermore, high abundance of it might be its higher enrichment during garbage decomposition in this study. In addition, unclassified_*Didymosphaeriaceae*, *Talaromyces*, *Rigidoporus*, *Mortierella*, *Ustilago*, *Phanerochaete*, *Myrmecridium* and unclassified_Fungi were also found in this study. Among hundreds of *Talaromyces* species, *Talaromyces* (*Penicillium*) *marneffei* is the pathogen for mammals, including humans, and as a primary lung pathogen, it disseminates to other internal organs for manipulating host immune cells (Pruksaphon et al., 2022). These airborne genera contained pathogens that inevitably increase human exposure risks of bioaerosols in the building with/without semi-open settings.

4.3. Building bio-pollution of city public sanitation scenarios

Among the building bio-pollution results of city public restrooms, it comparatively verified the airborne bioaerosol pollution differences in the restrooms with different building parameters, including building structures with/without semi-open settings and building coverage ratio. As reported, for RH at 40 %–60 % indoors, ventilation rate provides an impact on reducing airborne levels of SARS-CoV-2 than increasing indoor atmospheric RH (Aganovic et al., 2021). In this study, there was a higher risk of inhaling pathogens in buildings because of lower RH (20 %)-induced finer bioaerosol potential for human exposures, owing to the building structure with closed restrooms. Further, the study indicates that the atmospheric RH can affect the airborne particles' components and microbial communities dispersing from the public restrooms.

Some studies have shown that the interactions between complex meteorological conditions and pathogen pollution have a direct effect on building public restroom bio-pollution (Gong et al., 2020; Zhang et al., 2024). Quantitative techniques can utilize numerical data and mathematical models to forecast future value of a variable outcomes, whereas qualitative scenarios can be enriched by showing trends and dynamics (Booth et al., 2016). Therefore, in the future, the simulation of bioaerosol diffusion in the humid wind of high-density tall building areas should be carried out to disclose the intensifying effects on the atmospheric mixing and local area accumulation of pathogenic bioaerosol emissions.

5. Conclusion

This study proposed a residential building cluster model method for determining the bioaerosol diffusion concentration differences in Southern and Northern China cities based on field-measured and wind-tunnel-measured data. A simplified modeling of a high-rise building complex was investigated with a consideration of the surrounding area as a means of evaluating the dispersion profiles in building restrooms.

Humid wind contributes to greater atmospheric turbulence and mixing along the passage of the lower floors of the seven-floor mid-rise buildings with open settings for restrooms of the Southern China buildings with high building coverage ratios in this study. This monitoring resulted in a longer transmission distance of high-concentration 2.1–3.3 μm inhalable bioaerosols along the passages outside public restrooms. The results also verified that the dry air turbulent flow pattern in the passages of the seven-floor buildings with closed settings of restrooms dominated the diffusion of $<$1.1 μm bioaerosols and their long-time residence in the Northern China buildings. The modelling further confirmed the facts of the diffused bioaerosol distribution changes in the regional atmospheric winds and mutually corroborated with the explicable concentration decreasing gradients of culturable pathogenic bacteria bioaerosols from the newly-proposed wind tunnel experiments.

In the buildings' public restrooms, the abundant airborne culturable pathogens emerged, including *Staphylococcus aureus* and *Aspergillus fumigatus*. The accumulations of pathogenic bioaerosols changed significantly in the areas of high/low building coverage ratios. Furthermore, this study can inform us of the potential health risk of the restroom diffused human gut related pathogenic bioaerosols, including *E. coli* bioaerosols. This study can support decision-making to reduce bioaerosol potential for increased exposure, and then highlight the public sanitation protection and health risk management. Further works will endeavor on dynamic public restroom hygiene situations in a user interface modelling based on population streams in city buildings.

CRediT authorship contribution statement

Ting Zhang: Writing – original draft, Methodology, Investigation. **Zuming Wang:** Methodology, Data curation. **Simeng Zhang:** Methodology, Formal analysis. **Yuying Chen:** Validation. **Guiying Li:** Writing – review & editing, Conceptualization. **Taicheng An:** Supervision, Conceptualization.

Declaration of competing interest

The authors declare that they have no known competing financial interests or personal relationships that could have appeared to influence the work reported in this paper.

Acknowledgements

This work was supported by National Key Research and Development Program of China (2023YFC3708204), Guangdong-Hong Kong-Macao Joint Laboratory Corporation Foundation (GHMJLCEH-02), National Natural Science Foundation of China (42130611 and 42007385), the Natural Science Foundation of Liaoning Provincial, China (2023-MS-316), and the Liaoning Technical University Talent Foundation, China (21–1144).

Appendix B. Supplementary data

Supplementary data to this article can be found online at https://doi.org/10.1016/j.envpol.2025.127283.

Data availability

No data was used for the research described in the article.

References

Aganovic, A., Bi, Y., Cao, G., Drangsholt, F., Kurnitski, J., Wargocki, P., 2021. Estimating the impact of indoor relative humidity on SARS-CoV-2 airborne transmission risk using a new modification of the Wells-Riley model. Build. Environ. 205, 108278.

Ali, W., An, D.-z., Yang, Y.-f., Cui, B.-b., Ma, J.-x., Zhu, H., Li, M., Ai, X.-J., Yan, C., 2022. Comparing bioaerosol emission after flushing in squat and bidet toilets: quantitative microbial risk assessment for defecation and hand washing postures. Build. Environ. 221, 109284.

Alyousef, M., Alroqi, A., AlAmari, N., 2025. Atrophic rhinitis secondary to an infection of unusual bacteria: a case report and literature review. Ear Nose Throat J. 104, 162S–164S.

Anthamatten, L., von Bieberstein, P.R., Menzi, C., Zünd, J.N., Lacroix, C., de Wouters, T., Leventhal, G.E., 2024. Stratification of human gut microbiomes by succinotype is associated with inflammatory bowel disease status. Microbiome 12, 186.

Barbosa, C.G.G., Taylor, P.E., Sá, M.O., Teixeira, P.R., Souza, R.A.F., Albrecht, R.I., Barbosa, H.M.J., Sebben, B., Manzi, A.O., Araújo, A.C., Prass, M., Pöhlker, C., Weber, B., Andreae, M.O., Godoi, R.H.M., 2022. Identification and quantification of giant bioaerosol particles over the amazon rainforest. NPJ Clim. Atmos. Sci. 5, 73.

Booth, E.G., Qiu, J., Carpenter, S.R., Schatz, J., Chen, X., Kucharik, C.J., Loheide, S.P., Motew, M.M., Seifert, J.M., Turner, M.G., 2016. From qualitative to quantitative environmental scenarios: translating storylines into biophysical modeling inputs at the watershed scale. Environ. Model. Software 85, 80–97.

Božič, A., Kanduč, M., 2021. Relative humidity in droplet and airborne transmission of disease. J. Biol. Phys. 47, 1–29.

Braggion, A., Dugerdil, A., Wilson, O., Hovagemyan, F., Flahault, A., 2023. Indoor air quality and COVID-19: a scoping review. Public Health Rev. 44, 1605803.

Chen, D., Yan, J., Sun, N., Sun, W., Zhang, W., Long, Y., Yin, S., 2024a. Selective capture of PM2.5 by urban trees: the role of leaf wax composition and physiological traits in air quality enhancement. J. Hazard. Mater. 478, 135428.

Chen, Y., Liang, Z., Li, G., An, T., 2024b. Indoor/outdoor airborne microbiome characteristics in residential areas across four seasons and its indoor purification. Environ. Int. 190, 108857.

Chu, C.-R., Yang, K.-J., 2022. Transport process of outdoor particulate matter into naturally ventilated buildings. Build. Environ. 207, 108424.

Collings, K., Boisdon, C., Sham, T.-T., Skinley, K., Oh, H.-K., Prince, T., Ahmed, A., Pennington, S.H., Brownridge, P.J., Edwards, T., Biagini, G.A., Eyers, C.E., Lamb, A., Myers, P., Maher, S., 2023. Attaching protein-adsorbing silica particles to the surface of cotton substrates for bioaerosol capture including SARS-CoV-2. Nat. Commun. 14, 5033.

Csavina, J., Field, J., Félix, O., Corral-Avitia, A.Y., Sáez, A.E., Betterton, E.A., 2014. Effect of wind speed and relative humidity on atmospheric dust concentrations in semi-arid climates. Sci. Total Environ. 487, 82–90.

Dong, X., Chen, Z., Luo, Y., Wang, Z., Lin, Y., Su, J., 2024. Numerical investigation and dynamics of pollutant dispersion in underground restroom ventilation. J. Build. Eng. 88, 109132.

Douglas, P., Robertson, S., Gay, R., Hansell, A.L., Gant, T.W., 2018. A systematic review of the public health risks of bioaerosols from intensive farming. Int. J. Hyg Environ. Health 221, 134–173.

Erath, B.D., Ferro, A.R., 2022. Infectious disease transmission from bioaerosols. J. Expo. Sci. Environ. Epidemiol. 32, 645–646.

Fang, L., Ning, J., 2024. Recent advances in gut microbiota and thyroid disease: pathogenesis and therapeutics in autoimmune, neoplastic, and nodular conditions. Front. Cell. Infect. Microbiol. 14, 1465928.

Fu, N., Kim, M.K., Chen, B., Sharples, S., 2021. Investigation of outdoor air pollutant, PM2.5 affecting the indoor air quality in a high-rise building. Indoor Built Environ. 31, 895–912.

Ghosh, B., Lal, H., Srivastava, A., 2015. Review of bioaerosols in indoor environment with special reference to sampling, analysis and control mechanisms. Environ. Int. 85, 254–272.

Gollakota, A.R.K., Gautam, S., Santosh, M., Sudan, H.A., Gandhi, R., Sam Jebadurai, V., Shu, C.-M., 2021. Bioaerosols: characterization, pathways, sampling strategies, and challenges to geo-environment and health. Gondwana Res. 99, 178–203.

Gong, J., Qi, J., E, B., Yin, Y., Gao, D., 2020. Concentration, viability and size distribution of bacteria in atmospheric bioaerosols under different types of pollution. Environ. Pollut. 257, 113485.

Guo, K., Qian, H., Ye, J., Sun, F., Zhuge, Y., Wang, S., Liu, C., Cao, G., Zheng, X., 2021. Assessment of airborne bacteria and fungi in different-type buildings in Nanjing, a hot summer and cold winter moist Chinese city. Build. Environ. 205, 108258.

Gupta, A.D., Srivastava, V., Gupta, T., 2021. Seasonal bioaerosol load and statistical analysis within different microenvironments of an academic institute situated in the Indo-Gangetic Plain. Aerobiologia 37, 663–680.

Guyot, G., Sherman, M.H., Walker, I.S., 2018. Smart ventilation energy and indoor air quality performance in residential buildings: a review. Energy Build. 165, 416–430.

Hu, N., Yuan, F., Gram, A., Yao, R., Sadrizadeh, S., 2024. Review of experimental measurements on particle size distribution and airflow behaviors during human respiration. Build. Environ. 247, 110994.

Huyen, T.-T., Sekiguchi, K., Nghiem, T.-D., Ly, B.-T., 2024. Effect of indoor and outdoor emission sources on the chemical compositions of PM2.5 and PM0.1 in residential and school buildings. Air Qual. Atmos. Health 17, 1435–1450.

Ibrahim, S.R.M., Mohamed, H.M., Aljahdali, A.S., Murshid, S.S.A., Mohamed, S.G.A., Abdallah, H.M., Mohamed, G.A., 2025. *Aspergillus fumigatus* from pathogenic fungus to unexplored natural treasure: changing the concept. J. Microbiol. Biotechnol. 35, 1–24.

Kim, K.-H., Kabir, E., Jahan, S.A., 2018. Airborne bioaerosols and their impact on human health. J. Environ. Sci. (China) 67, 23–35.

Kraus, E.A., Prithiviraj, B., Hernandez, M., 2025. Advancing transcriptomic profiling of airborne bacteria. Appl. Environ. Microbiol. 0, e00148.

Lewis, A.C., Jenkins, D., Whitty, C.J.M., 2023. Hidden harms of indoor air pollution - five steps to expose them. Nature 614, 220–223.

Leylabadlo, H.E., Ghotaslou, R., Feizabadi, M.M., Farajnia, S., Moaddab, S.Y., Ganbarov, K., Khodadadi, E., Tanomand, A., Sheykhsaran, E., Yousefi, B., Kafil, H.S., 2020. The critical role of *Faecalibacterium prausnitzii* in human health: an overview. Microb. Pathog. 149, 104344.

Li, Q., Zhang, H., Cai, X., Song, Y., Zhu, T., 2021. The impacts of the atmospheric boundary layer on regional haze in North China. NPJ Clim. Atmos. Sci. 4, 9.

Lin, Q., Li, L., De Vrieze, J., Li, C., Fang, X., Li, X., 2023. Functional conservation of microbial communities determines composition predictability in anaerobic digestion. ISME J. 17, 1920–1930.

Liu, X., Huang, B., Li, R., Zhang, J., Gou, Q., Zhou, T., Huang, Z., 2022. Wind environment assessment and planning of urban natural ventilation corridors using GIS: shenzhen as a case study. Urban Clim. 42, 101091.

Liu, Z., Cao, H., Hu, C., Wu, M., Zhang, S., He, J., Jiang, C., 2023. Modeling the infection risk and emergency evacuation from bioaerosol leakage around an urban vaccine factory. NPJ Clim. Atmos. Sci. 6, 6.

Marin-Felix, Y., Hernández-Restrepo, M., Crous, P.W., 2020. Multi-locus phylogeny of the genus Curvularia and description of ten new species. Mycol. Prog. 19, 559–588.

Megahed, N.A., Ghoneim, E.M., 2021. Indoor air quality: rethinking rules of building design strategies in post-pandemic architecture. Environ. Res. 193, 110471.

Menekşe, Ş., Tanrıverdi, E.S., Altınay, E., Oğuş, H., Aydoğan, A.A., Sağlam, D., Çelik, Ö., Otlu, B., Kırali, M.K., 2023. A long-lasting *Sphingomonas paucimobilis* outbreak: a potential for pathogens to persist on environmental devices despite disinfection measures. Am. J. Infect. Control 51, 765–771.

Miletto, M., Lindow, S.E., 2015. Relative and contextual contribution of different sources to the composition and abundance of indoor air bacteria in residences. Microbiome 3, 61.

Morawska, L., Allen, J., Bahnfleth, W., Bennett, B., Bluyssen, P.M., Boerstra, A., Buonanno, G., Cao, J., Dancer, S.J., Floto, A., Franchimon, F., Greenhalgh, T., Haworth, C., Hogeling, J., Isaxon, C., Jimenez, J.L., Kennedy, A., Kumar, P., Kurnitski, J., Li, Y., Loomans, M., Marks, G., Marr, L.C., Mazzarella, L., Melikov, A. K., Miller, S.L., Milton, D.K., Monty, J., Nielsen, P.V., Noakes, C., Peccia, J., Prather, K.A., Querol, X., Salthammer, T., Sekhar, C., Seppänen, O., Tanabe, S.-i., Tang, J.W., Tellier, R., Tham, K.W., Wargocki, P., Wierzbicka, A., Yao, M., 2024. Mandating indoor air quality for public buildings. Science 383, 1418–1420.

Mubareka, S., Groulx, N., Savory, E., Cutts, T., Theriault, S., Scott, J.A., Roy, C.J., Turgeon, N., Bryce, E., Astrakianakis, G., Kirychuk, S., Girard, M., Kobinger, G., Zhang, C., Duchaine, C., 2019. Bioaerosols and transmission, a diverse and growing community of practice. Front. Public Health 7, 23.

Myers, N.T., Calderón, L., Pavilonis, B., Wang, Z., Xiong, Y., Sorensen-Allacci, M., Plotnik, D., Senick, J., Gong, J., Krogmann, U., Andrews, C.J., Mainelis, G., 2021. Presence and variability of culturable bioaerosols in three multi-family apartment buildings with different ventilation systems in the Northeastern US. Indoor Air 31, 502–523.

Obayori, O.S., 2023. Chapter 4 - indoor and outdoor aeromicrobiology. In: Ilori, M.O., Obayori, O.S., Salam, L.B. (Eds.), Aeromicrobiology. Academic Press, pp. 59–88.

Ota, M., Takahara, S., Yoshimura, K., Nagakubo, A., Hirouchi, J., Hayashi, N., Abe, T., Funaki, H., Nagai, H., 2023. Soil dust and bioaerosols as potential sources for resuspended 137Cs occurring near the Fukushima Dai-ichi nuclear power plant. J. Environ. Radioact. 264, 107198.

Peng, L., Peng, C., Li, G., An, T., 2025. A critical mini-review on atmospheric ozone mediated alterations of bioaerosols and their effects on human health. Global Environ. Sci. 1, 36–43.

Pietsch, R.B., Grothe, H., Hanlon, R., Powers, C.W., Jung, S., Ross, S.D., Schmale Iii, D.G., 2018. Wind-driven spume droplet production and the transport of *Pseudomonas syringae* from aquatic environments. PeerJ 6, e5663.

Pöhlker, M.L., Pöhlker, C., Krüger, O.O., Förster, J.D., Berkemeier, T., Elbert, W., Fröhlich-Nowoisky, J., Pöschl, U., Bagheri, G., Bodenschatz, E., Huffman, J.A., Scheithauer, S., Mikhailov, E., 2023. Respiratory aerosols and droplets in the transmission of infectious diseases. Rev. Mod. Phys. 95, 045001.

Pruksaphon, K., Nosanchuk, J.D., Ratanabanangkoon, K., Youngchim, S., 2022. *Talaromyces marneffei* infection: virulence, intracellular lifestyle and host defense mechanisms. J. Fungi (Basel) 8, 200.

Qi, J., Li, M., Zhen, Y., Wu, L., 2018. Characterization of bioaerosol bacterial communities during hazy and foggy weather in Qingdao, China. J. Ocean Univ. China 17, 516–526.

Ravi, S., D'Odorico, P., 2005. A field-scale analysis of the dependence of wind erosion threshold velocity on air humidity. Geophys. Res. Lett. 32, L21404.

Ren, W., Feng, Z., Wang, X., Li, Y., Long, H., Cai, X., Huang, A., Xie, Z., 2023. Contribution of the types of tropical coastal aquaculture ponds to the differential distribution of the family bacillaceae bacterial community. Aquac. Res. 2023, 4522234.

Sui, X., Tian, Z., Liu, H., Chen, H., Wang, D., 2021. Field measurements on indoor air quality of a residential building in Xi'an under different ventilation modes in winter. J. Build. Eng. 42, 103040.

Tseng, C.-H., Wang, H.-C., Xiao, N.-Y., Chang, Y.-M., 2011. Examining the feasibility of prediction models by monitoring data and management data for bioaerosols inside office buildings. Build. Environ. 46, 2578–2589.

Violaki, K., Nenes, A., Tsagkaraki, M., Paglione, M., Jacquet, S., Sempéré, R., Panagiotopoulos, C., 2021. Bioaerosols and dust are the dominant sources of organic P in atmospheric particles. NPJ Clim. Atmos. Sci. 4, 63.

Wang, C.C., Prather, K.A., Sznitman, J., Jimenez, J.L., Lakdawala, S.S., Tufekci, Z., Marr, L.C., 2021. Airborne transmission of respiratory viruses. Science 373, eabd9149.

Wu, J., 1981. Evidence of sea spray produced by bursting bubbles. Science 212, 324–326.

Xie, Z., Fan, C., Lu, R., Liu, P., Wang, B., Du, S., Jin, C., Deng, S., Li, Y., 2018. Characteristics of ambient bioaerosols during haze episodes in China: a review. Environ. Pollut. 243, 1930–1942.

Yu, Y., Liang, Z., Liao, W., Ye, Z., Li, G., An, T., 2021. Contributions of meat waste decomposition to the abundance and diversity of pathogens and antibiotic-resistance genes in the atmosphere. Sci. Total Environ. 784, 147128.

Zhang, S., Liang, Z., Wang, X., Ye, Z., Li, G., An, T., 2023a. Bioaerosols in an industrial park and the adjacent houses: dispersal between indoor/outdoor, the impact of air purifier, and health risk reduction. Environ. Int. 172, 107778.

Zhang, T., Chen, Y., Cai, Y., Yu, Y., Liu, J., Shen, X., Li, G., An, T., 2023b. Abundance and cultivable bioaerosol transport from a municipal solid waste landfill area and its risks. Environ. Pollut. 320, 121038.

Zhang, T., Chen, Y., Li, G., 2025. Synergistic effects of the urban-rural divide on outdoor airborne bioaerosol diffusion: a case study in the monsoon region of China. Global Environ. Sci. 1, 3–18.

Zhang, T., Li, G., Yu, Y., Ji, Y., An, T., 2020. Atmospheric diffusion profiles and health risks of typical VOC: numerical modelling study. J. Clean. Prod. 275, 122982.

Zhang, T., Zhang, D., Lyu, Z., Zhang, J., Wu, X., Yu, Y., 2024. Effects of extreme precipitation on bacterial communities and bioaerosol composition: dispersion in urban outdoor environments and health risks. Environ. Pollut. 344, 123406.

Zhou, X., Simha, P., Perez-Mercado, L.F., Barton, M.A., Lyu, Y., Guo, S., Nie, X., Wu, F., Li, Z., 2022. China should focus beyond access to toilets to tap into the full potential of its rural toilet revolution. Resour. Conserv. Recycl. 178, 106100.